Upcycling Watermelon Peel Waste into a Sustainable Environment-Friendly Biochar for Assessment of Effective Adsorption Property

Ziyu Yuan[1] · Xingxing Sun[2] · Jiayi Hua[2] · Yao Zhu[2] · Junjie Yuan[1] · Fengxian Qiu[2]

Abstract

Recently, the utilization of peel waste is a significant topic of resource recycling and environment protection. Watermelon is one of the most important fruit species in the world, and its peel accounts for nearly 30% of the weight of watermelon. Here, a series of biochar (WB) derived from watermelon peel and modified biochar (MWB) materials using KOH modifier as adsorbents were successfully prepared with slow pyrolysis at different temperatures (400, 500, 600 and 700 °C). The structure, morphology and specific surface area of the biochar materials were characterized and measured. The optimum adsorption removal conditions of chromium ion (VI) ion from aqueous solution were investigated. The prepared biochar adsorbents had excellent adsorption performance toward Cr(VI) pollutants. The kinetics, isotherm and thermodynamic adsorption process of system were studied. The obtained results indicated that adsorption systems were well followed by pseudo-second-order equation, the Langmuir model (104.17 mg/g of maximum adsorption capacity), endothermic and spontaneous. The recycling experiment demonstrated that the removal efficiency of the optimal material was 85% after 5 cycles. Hence, the prepared modified MWB material is not only helpful to solve the management problem of waste watermelon peel, but also can obtain environment-friendly final green products with potential commercial value.

1 Introduction

With the development of industry, toxic dyes, organic pharmaceuticals drugs, heavy metals and other pollutants in the aquatic environment are discharged into water resources such as ponds, lakes, streams, rivers and oceans, seriously affecting the quality of environmental water resources [1–5]. When heavy metal (e.g., chromium ion, lead ion, cadmium ion, etc.) pollutants in water exceed the maximum allowable limit, they will cause toxic effects and diseases [6, 7]. For example, chromium is a highly reactive metal and exists in various oxidation states in aqueous solutions (II, III, VI). The chromium (VI) compounds have carcinogenic effects and also can lead to many other health problems, such as epistaxis, ulcer and perforation of nasal septum. The threshold value for Cr(VI) has been reported 1 mg/L [8]. Therefore, it is necessary to develop economic and environmental-friendly technology removal of chromium ion (VI) in liquid waste [9–11].

In recent years, many traditional separation technologies were reported, such as membrane separation, ion exchange, solvent extraction, electrochemical treatment and adsorption [12–14]. From the reported technology, the adsorption method has the advantages of high efficiency, low cost and convenient treatment. Biochar obtained from agricultural waste, biological waste and peel waste can be used as adsorbents to remove metal pollution in environmental water resources. These adsorbents are much cheaper and environmentally friendly in nature. Rajapaksha et al. prepared biochars with soybean and burcucumber residues as raw materials and studied the removal chromium (VI) ion [15]. Shakya and Agarwal prepared four kinds of biochar by slow pyrolysis of pineapple peel waste and investigated their removal characteristics of Cr(VI) from water [16]. Pap

✉ Junjie Yuan
  yuanjunjie@ujs.edu.cn

✉ Fengxian Qiu
  fxqiu@ujs.edu.cn

1 School of Agricultural Engineering, Jiangsu University, Zhenjiang 212013, China

2 School of Chemistry and Chemical Engineering, Jiangsu University, Zhenjiang 212013, China

et al. reported that biochars were prepared from plums and apricots fruit waste and investigated their removal abilities of chromium and lead ions [17]. However, due to poor adsorption performance and unsatisfactory recovery process, the practical application and treatment of these biochar will be limited. In recent years, there have been a series of studies on the modification of biochar. The modification methods include alkali or acid treatment, metal salt impregnation, gas activation and UV modification [18–22].

In summer, watermelon is the most popular and best-selling fruit in the Chinese fruit market. Its skin is usually discarded and treated as waste. Without timely and appropriate treatment, a large number of peels will accumulate in nature, rot and pollute the environment. Therefore, using fruit peel as raw material to prepare biochar is an eco-friendly protection method to solve its disposal problem. In this work, biochar from watermelon peel was prepared and applied to remove chromium ion (VI). Moreover, KOH was used as modifier in the production of biochar. The objectives summarized as follows: (a) characterize the morphology and structure of biochar prepared at different the pyrolysis temperature; (b) investigate the mechanism of Cr(VI) adsorption; (3) discuss Cr(VI) adsorption process by adsorption kinetics, thermodynamics and isotherm; (4) measure regeneration performance of the adsorbent. This work can provide a new method for peel waste biochar preparation and Cr(VI) removal.

2 Experimental Section

2.1 Reagents and Raw Material

Watermelon peels were obtained from the fruit market. Potassium hydroxide (KOH) and potassium dichromate ($K_2Cr_2O_7$) were provided by Sinopharm Chemical Reagent Co. Ltd. (China). Synthetic stock chromium solution (1000 mg/L) was prepared by dissolving $K_2Cr_2O_7$ (2.829 g) in 1000 mL deionized water.

2.2 Preparation of Modified Biochar

The waste watermelon peel was collected, washed, dried at 80 °C for 12 h and crushed to obtain watermelon peel powder (WPP). Then, WPP (3.6 g) was introduced into a muffle furnace in ceramic cups and heated at different desired temperatures (400, 500, 600 and 700 °C) for 3 h. Following pyrolyzation, the produced biochar (WB) was cooled, washed and dried at temperature of 105 °C for 2.5 h. The WB was sieved ($\leq 200~\mu m$) and stored in a sealed bottle for further experiments and referred as WB-400, WB-500, WB-600 and WB-700 according to their pyrolysis temperatures.

To prepare the KOH modified biochars, the WPP was mixed with KOH powder (mass ratio of 1.00:1.55) and then was introduced into a muffle furnace in ceramic cups and heated at different desired temperatures (400, 500, 600 and 700 °C) for 3 h. Then, the powder was washed with sodium hydroxide (0.1 M) and ultrapure water and dried at temperature of 105 °C for 2.5 h [23]. The KOH modified biochars were sieved ($\leq 200~\mu m$) and labeled MWB-400, MWB-500, MWB-600 and MWB-700, respectively. A series of WB and MWB materials as adsorbents were applied to remove chromium ion (VI) from aqueous solutions. The preparation and adsorption process are shown in Scheme 1.

2.3 Instruments

Fourier transform infrared spectrum (FT-IR) was obtained from AVATAR 360 spectrometer in the wave number range from 4000 to 400 cm^{-1}. Scanning electron microscopy was obtained from SEM Hitachi S-4800. X-ray diffraction (XRD) was conducted on Shimadzu XRD-6100. The specific surface area and the pore diameter distributions were calculated from a Micromeritics TriStar II 3020 analyzer.

2.4 Batch Adsorption Experiments

Batch experiments were carried out with respect to different adsorption conditions. After equilibrium, the solution was filtered and concentration of Cr(VI) was measured with UV-2450 spectrophotometer at 540 nm by using 1,5-diphenylcarbohydrazide (DPC) method. The removal rate (R, %) of Cr(VI) was calculated by Eq. (1):

$$R = \frac{(C_0 - C_e)}{C_0} \times 100\% \tag{1}$$

where C_0 and C_e (mg/L) are the initial and equilibrium concentration of Cr(VI) in the solution, respectively [24, 25].

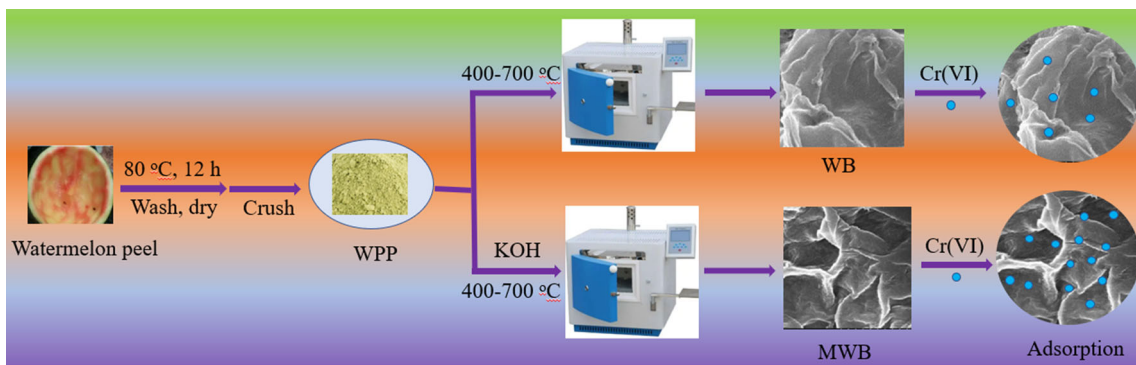The adsorption capacity was calculated by following Eq. (2):

$$Q_e = \frac{(C_0 - C_e)}{M} \times V \tag{2}$$

where Q_e is the adsorption capacity (mg/g) of WB or MWB, M is the mass (g) of WB or MWB, and V is the volume (L) of solution.

3 Results and Discussion

3.1 Characterization of WB and MWB

FT-IR spectra of WB and MWB are presented in Fig. 1. From Fig. 1a, the broad absorption band in the range
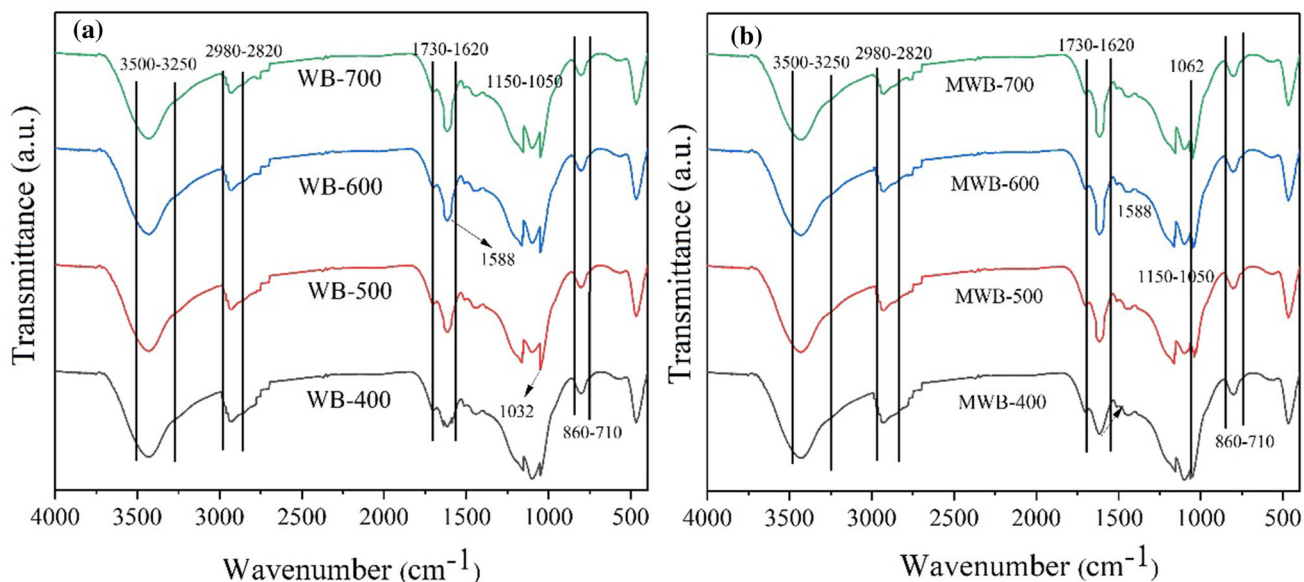
Scheme 1 The preparation and adsorption process

Fig. 1 FT-IR spectra of biochar (**a**) and modified biochar (**b**) materials

3250–3500 cm^{-1} was the stretching vibration of hydroxyl groups. The characteristic absorption peak located at around 1050–1150 cm^{-1} was attributed to the celluloses and hemicelluloses of polysaccharides [22]. The absorption band in the range 2980–2820 cm^{-1} was the stretching vibration (C–H) of aliphatic groups and was also observed that the high pyrolysis temperature weakened the intensity. This phenomenon may be due to the demethoxylation, demethylation and dehydration of lignin to form unstable aliphatic compounds during the preparation of biochar [26]. The stretching vibration at 1620–1730 cm^{-1} was appeared to the –C=O stretching peak of WB. The band at 1032 cm^{-1} was attributed to the C–O and C–O–C stretching vibration peaks. The peak at 1588 cm^{-1} was assigned to the aromatic = O and C=C groups, and with the increase of pyrolysis temperature, its intensity was also gradually increasing. The bands at 710–860 cm^{-1} were the C–H and/or C–O aryl groups. At lower pyrolysis temperatures (400 °C), due to partial chemical conversion under these conditions, the behavior

of biochar was similar to that of raw materials that maintained a certain hydration and carbohydrate structure [27]. From Fig. 1b, the stretching vibration of C–O was observed at 1062 cm^{-1} [28]; the above corresponding bands of biochars also appeared in the modified biochar materials.

XRD results of WB (a) and MWB (b) materials are presented in Fig. 2. In Fig. 2a, the characteristic peaks of all WB and MWB materials at $24.5°$ and $43.9°$ were designated as amorphous carbon (JCPDS No. 50-0926). When the biochar was modified with KOH, the new phase of K_2O can be observed at $29.6°$, $32.2°$ and $51.9°$ [29] (JCPDS 00-019-0927), and with the increase of pyrolysis temperature, its intensity was also gradually increasing (Fig. 2b).

The pyrolysis temperature affects the morphology and pore structure. SEM images of WB-400 (a), WB-500 (b), WB-600(c), MWB-700 (d), MWB-400 (e), MWB-500 (f), MWB-600 (g) and MWB-700 (h) materials are shown in Fig. 3. As shown in Fig. 3a, b, c and d, the original structure of the biochar was changed little at lower pyrolysis
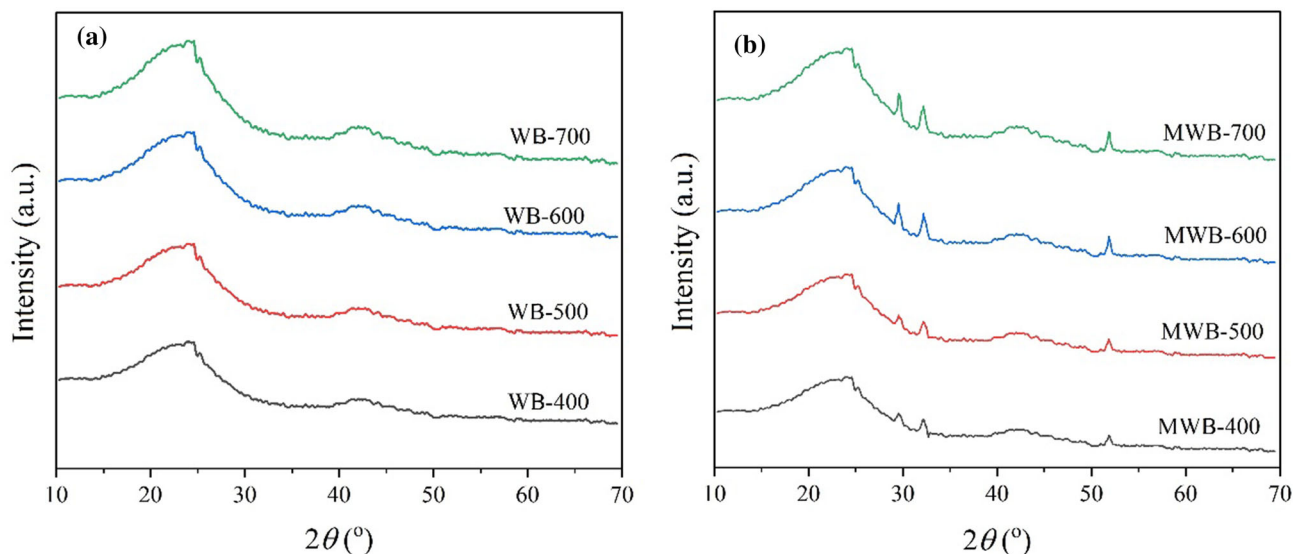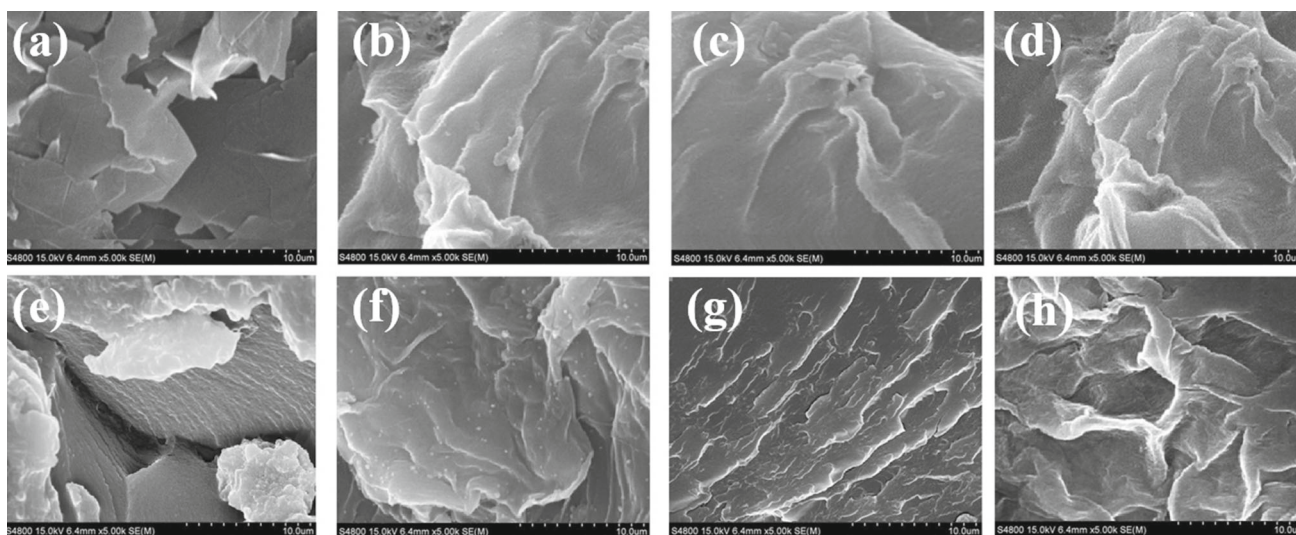
Fig. 2 XRD patterns of biochar (**a**) and modified biochar (**b**) materials

Fig. 3 SEM images of WB-400 (**a**), WB-500 (**b**), WB-600 (**c**), MWB-700 (**d**), MWB-400 (**e**), MWB-500 (**f**), MWB-600 (**g**) and MWB-700 (**h**) materials

temperature, showing that the inherent molecular structure of biomass (i.e., lignin, hemicellulose and crystalline cellulose) could be retained [30]. The graphite sheet structure was observed at higher pyrolysis temperature. This is mainly due to the delocalized π bonds caused sp^2 hybridization [22]. From Fig. 3e, f, g and h, the pore structure was displayed after KOH modification, which would be conducive to the adsorption of chromium.

The influences of pyrolysis temperature on the average pore of WB and MWB materials are summarized in Table 1. With the increase of pyrolysis temperature, the BET specific surface area was also gradually increasing. This was mainly because the aliphatic carboxyl group was disintegrated (as evidenced by the FT-IR spectrum in Fig. 1) and the lignin

Table 1 The BET specific surface area and average pore of WB and MWB materials

Samples	Specific surface area (m^2/g)	Average pore diameter (nm)
WB-400	5.56	1.04
WB-500	26.25	1.26
WB-600	78.88	1.58
WB-700	70.54	1.44
MWB-400	35.26	1.48
MWB-500	100.23	1.98
MWB-600	132.27	2.57
MWB-700	126.05	2.08

aromatic nuclei was bared. However, in all biochars and modified biochar materials, MWB-600 had the highest BET area and pore. This may be due to the raise of micropores after removal of volatiles. Interestingly, the specific surface area and pore diameter decreased slightly as the temperature increased from 600 to 700 °C, which may be considered to be caused by the pore's shrinkage and the microporous wall's collapse. However, the structural deformation caused by the accumulation of adjacent pores, as well as the softening, melting and pore blockage formed by melting of ash, may make the surface area lower at higher pyrolysis temperature [15]. From Table 1, at the same pyrolysis temperature, the specific surface areas of MWB series (after KOH modification) were bigger than those of WB series. This may be because KOH modifier can react with the carboxyl group in watermelon peel biochar, which accelerated the formation of porous structure of modified biochars with the increase of pyrolysis temperature. Moreover, the relative average pore diameter of MWB series (after KOH modification) was bigger than those of WB series, which was in favor of the effective removal of Cr(VI). This was mainly because KOH modifier is helpful to the formation of micropores in the obtained MWB materials [23]. WB-600 and MWB-600 materials were selected as performance comparison in the next experiments.

3.2 Study on Adsorption Conditions

pH value of the solution is an important factor affecting the adsorption Cr(VI) ion process. It could control the surface charge and ion state of the prepared biochar surface functional groups, and also have a certain impact on the existing species and redox potential of Cr (VI) in the adsorption system. To explore the optimal pH value of WB-600 and MWB-600 materials for the adsorption of Cr (VI), the influence of solution pH value on the removal rate of Cr(VI) was investigated under the conditions of 25 °C, 2 ~ 11 of pH value, 150 mg/L of initial concentration and time of 8 h. HCl or NaOH solutions (0.1–1 M) were used for pH adjustment. The obtained results of pH on the removal rate of Cr(VI) and zeta potential of WB-600 and MWB-600 materials are presented in Fig. 4a, b. From Fig. 4a, the removal rate of Cr(VI) by WB-600 and MWB-600 materials reached a maximum removal rate of 89.42% for WB-600 and 92.76% for MWB-600 at pH 3, respectively. The removal rate progressively decreased with the increase of pH from 3.0 to 9.0. This may be because Cr (VI) existed in various forms (e.g., CrO_4^{2-}, H_2CrO_4, $Cr_2O_7^{2-}$ and $HCrO_4^-$) in aqueous solution. The distribution of Cr (VI) species is dependent on both the total concentration of Cr (VI) and pH of the equilibrium solution. Following Eqs. (3), (4) and (5) describe the distribution of

chromium species in aqueous solution [31]:

$$H_2CrO_4 \leftrightarrow HCrO_4^- + H^+ \tag{3}$$

$$HCrO_4^- \leftrightarrow CrO_4^{2-} + H^+ \tag{4}$$

$$2HCrO_4^- \leftrightarrow Cr_2O_7^{2-} + H_2O \tag{5}$$
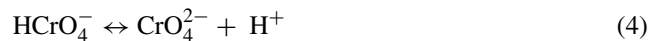
At pH < 3, $Cr_2O_7^{2-}$ was the main form of Cr (VI), while $HCrO_4^-$ and $Cr_2O_7^{2-}$ were the main forms at pH 2–6 and CrO_4^{2-} dominated at pH > 6 [23]. In other words, the CrO_4^{2-} anion prevailed in basic or slightly acidic solution, while the $Cr_2O_7^{2-}$ anion was dominant in acidic Cr (VI) aqueous solution [31]:

$$CrO_4^{2-} (pH > 6) \leftrightarrow HCrO_4^{2-} (pH\ 2 - 6) \leftrightarrow Cr_2O_7^{2-} (pH < 3) \tag{6}$$
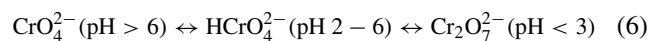
In this work, with pH changing from 3 to 9, the removal rate of Cr(VI) declined from 89.42 ± 0.09% to 10.42 ± 0.18% for WB-600, while the removal rate of Cr(VI) declined from 92.76 ± 0.17% to 18.31 ± 0.08% for MWB-600. These results revealed that WB-600 and MWB-600 materials had excellent adsorption removal Cr(VI) under acidic environment. At lower pH, the surface of biochar was positively charged due to the protonation of some groups. Thus, electrostatic attraction was generated between biochar and chromium oxygen anion [16]. The increase of pH value leaded to the deprotonation of some groups, so as to form an electronegative surface and reduce the retention of Cr (VI) species. When the pH of the solution was greater than 6, the adsorption Cr (VI) can be ignored due to the competitive effect between OH^- ion and chromium ion on the adsorption site. In addition, at higher pH value, the electrostatic repulsion between chromate ions and negatively charged on the biochar surface would also reduce the removal rate of Cr (VI) to a great extent. These results showed that in acidic solution, electrostatic interaction played a key role in the adsorption of Cr (VI), while in alkaline solution, it was mainly the complexation of ions. To further confirm the electrostatic interaction effect on the Cr(VI) adsorption, the pHzpc values of WB-600 and MWB-600 materials were tested, as shown in Fig. 4b. As indicated from Fig. 4b, the pHpzc (9.58) of MWB-600 material was higher than that (8.09) of WB-600 material, and these results could support the above analysis. These measured pHpzc values were close to the previously reported results of biomass carbon and alkali-modified biomass carbon [16, 32]. This also may be that the alkalinity of the material was enhanced after KOH modification. Therefore, pH = 3 was selected in this work.

Effect of WB-600 and MWB-600 materials dosage on the removal rate of Cr(VI) is presented in Fig. 5. From Fig. 5, with the increase of the WB-600 and MWB-600 materials
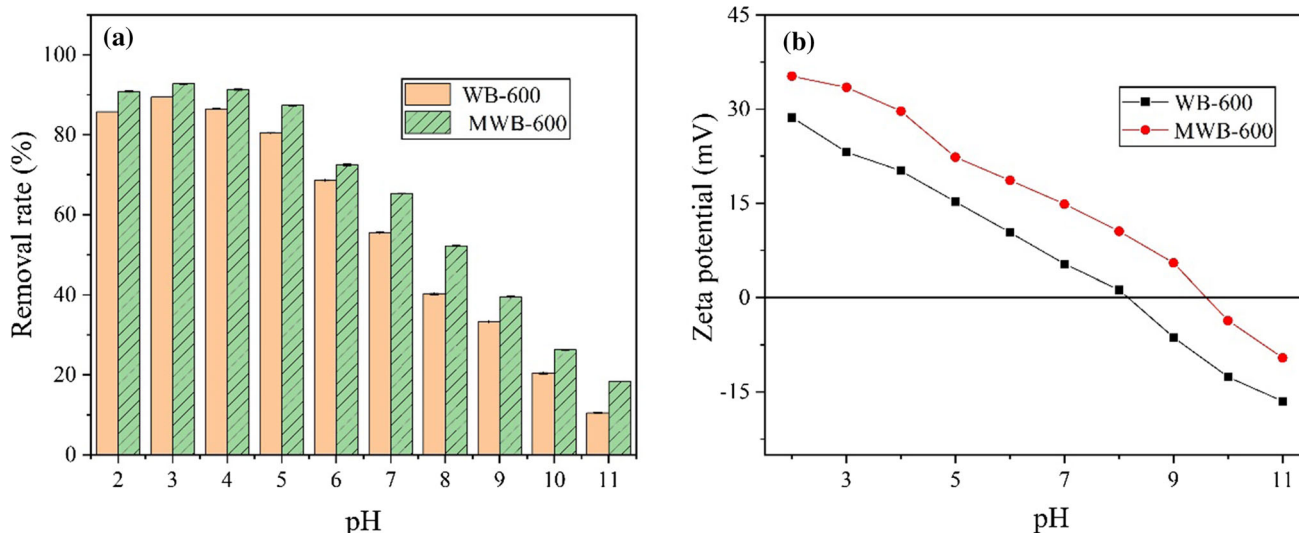
Fig. 4 Effect of different pH on the Cr(VI) adsorption (**a**) and zeta potential (**b**) of WB-600 and MWB-600 materials (Cr(VI) solution: 150 mg/L, adsorbent dosage: 2.0 g/L, *T*: 25 °C, *t*: 8 h)
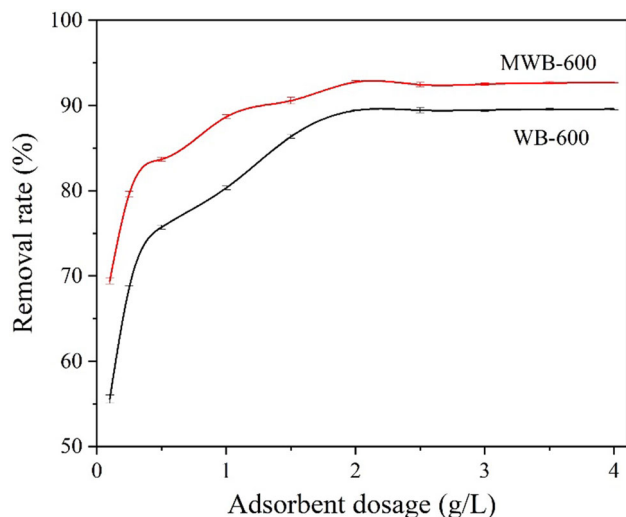

Fig. 5 Effect of WB-600 and MWB-600 materials dosage on Cr(VI) removal rate (Cr(VI) solution: 150 mg/L, pH: 3.0, *T*: 25 °C, *t*: 8 h)

dosage, the removal rate of Cr(VI) progressively increased. This was mainly divided into two growth stages. With dosage of WB-600 and MWB-600 materials changing from 0.5 to 2.0 g/L, the removal rate of Cr(VI) increased rapidly. This was because at this stage, the solution contained enough Cr (VI) and the active sites on WB-600 and MWB-600 materials can be completely adsorbed. The second stage was the dosage of WB-600 and MWB-600 materials changing from 2.0 to 4.0 g/L, and Cr (VI) removal rate changed little. This may be that the amount of Cr (VI) was not enough, but the adsorption active site was enough, resulting in little change in the adsorption rate of chromium. When the amount of MWB-600 adsorbent was 2.0 g/L, the removal rate of Cr (VI)

reached the maximum, 92.76%. Considering the general situation of adsorption process, the optimal dosage of biochar and modified biochar material was selected to 2.0 g/L in this work.

3.3 Adsorption Isotherm, Kinetics Models and Thermodynamic Study

The linear form of the Langmuir isotherm model equation is presented by Eq. (7):

$$\frac{1}{q_e} = \frac{1}{q_m} + \frac{1}{K_L q_m C_e} \tag{7}$$

where q_e is the adsorption capacity at adsorption equilibrium (mg/g), q_m is maximum adsorption capacity (mg/g), C_e is the equilibrium concentration (mg/L), and K_L is the Langmuir binding constant (L/mg) [33–35].

The linear form of the Freundlich isotherm model is presented by Eq. (8):

$$\ln q_e = \ln K_f + \frac{1}{n} \times \ln c_e \tag{8}$$

where K_f is the Freundlich adsorption constant [(mg/g) (L/mg)$^{1/n}$]; C_e is the equilibrium concentration (mg/L) [33].

The fitting results are presented in Fig. S1, S2 and Table 2. From Table 2, the correlation coefficient (R^2) of Langmuir model was 0.9950–0.9994, and the fitting results were consistent with the experimental data. The correlation coefficients of the Langmuir isothermal model were bigger than those of Freundlich isothermal model. The obtained results showed that the Langmuir model was more appropriate than Freundlich model [36], indicating that the specific binding

Table 2 Comparison of Langmuir and Freundlich isotherm models

Model	Material	Parameter	25 °C	35 °C	45 °C
Langmuir	WB-600	q_m (mg/g)	83.61	89.85	99.60
		K_L (L/mg)	0.0296	0.0352	0.0353
		R^2	0.9994	0.9989	0.9992
	MWB-600	q_m (mg/g)	85.54	95.51	104.17
		K_L (L/mg)	0.0349	0.0371	0.0405
		R^2	0.9943	0.9981	0.9993
Freundlich	WB-600	K_f ((mg/g) (L/mg)$^{1/n}$)	1.8435	2.6439	2.8482
		$\frac{1}{n}$	1.2973	1.2598	1.2761
		R^2	0.9950	0.9989	0.9904
	MWB-600	K_f ((mg/g) (L/mg)$^{1/n}$)	2.1384	2.7867	3.7657
		$\frac{1}{n}$	1.3495	1.3067	1.2398
		R^2	0.9596	0.9837	0.9971

sites for Cr(VI) were homogeneously distributed on the material surface, and the binding toward Cr(VI) was a monolayer adsorption. The maximum q_m values of WB adsorbent were 83.61, 89.85, 99.60 mg/g, while q_m values of MWB adsorbent were 85.84, 95.51, 104.17 mg/g at temperatures of 25, 35 and 45 °C, respectively. As indicated in Table 2, the maximum q_m value of MWB-600 material was higher than that of WB-600 material at the same temperature. This should be attributed to the results of KOH modification.

Pseudo-first-order and pseudo-second-order model equations are presented by Eqs. (9) and (10).

$$\ln(q_e - q_t) = \ln q_e - K_1 t \tag{9}$$

$$\frac{t}{q_t} = \frac{1}{K_2 q_e^2} + \frac{t}{q_e} \tag{10}$$

where q_e (mg/g) and q_t (mg/g) are the adsorption capacities of Cr(VI) on the biochar and modified biochar materials at equilibrium and time t (min), respectively. K_1 and K_2 are the adsorption rate constants for the pseudo-first-order model and pseudo-second-order model, respectively [24, 35].

Corresponding plots for the models are shown in Fig. S3, S4 and Table 3. As equations and R^2 in the plots show, the results can be well modeled by the pseudo-second-order kinetics model ($R^2 > 0.9998$) for describing the kinetics of the process. This confirmed that the overall process depended on the amount of Cr(VI) in contacting solution and the availability of adsorption sites on WB-600 and MWB-600 [23].

The thermodynamic experiments studies of WB-600 and MWB-600 adsorbents were conducted at different temperatures and the Cr(VI) concentration of 150 mg/L. The distribution coefficient, K_c, was calculated using Eq. (11).

$$K_c = \frac{C_o - C_e}{C_e} = \frac{q_e M}{C_e V} \tag{11}$$

where C_0, C_e, M and V are the initial concentration, equilibrium (mg/L), the mass of the WB-600 or MWB-600 (g) and volume of the solution (mL), respectively.

Adsorption thermodynamics is important for describing the adsorption properties of sorbents, and $\Delta G°$, $\Delta H°$ and $\Delta S°$ are the main parameters which can be calculated by following Eqs. (12), (13) and (14):

$$\Delta G^o = -RT \ln K_c \tag{12}$$

$$\Delta G^o = \Delta H^o - T1S^o \tag{13}$$

$$\ln K_c = -\frac{\Delta H^o}{RT} + \frac{\Delta S^o}{R} \tag{14}$$

where $\Delta G°$, $\Delta H°$, $\Delta S°$, R and T values are Gibbs free energy (kJ/mol), enthalpy (kJ/mol), entropy (J/mol·K), the gas constant (8.314 J/(mol·K)) and the absolute temperature (K), respectively.

The values of ΔS and ΔH can be calculated from its intercept and slope, respectively (see Fig. S5, Supporting Information). According to the obtained results, $\Delta H°$ and $\Delta S°$ values were 66.30 kJ/mol and 14.43 J/mol K for WB-600 adsorbent, while $\Delta H°$ and $\Delta S°$ values were 28.56 kJ/mol and 2.20 J/mol K for MWB-600 adsorbent, respectively. The $\Delta G°$ values (− 5.33 kJ/mol (25 °C), − 5.99 kJ/mol (35 °C), − 6.65 kJ/mol (45 °C) for WB-600 adsorbent; and − 6.31 kJ/mol (25 °C), − 6.60 kJ/mol (35 °C), − 6.88 kJ/mol (45 °C) for MWB-600 adsorbent) were negative. As the results show, with increase in temperature ΔG became more negative, confirming that removal of Cr(VI) cations by the adsorbent was more favorable at higher temperatures because the process was an endothermic process ($\Delta H > 0$). Moreover, the positive $\Delta H°$ and $\Delta S°$ values indicated that Cr(VI) removal by both WB-600 and MWB-600 was endothermic
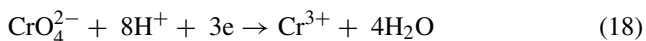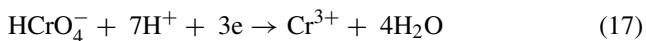
Table 3 The fitting parameters of kinetic model parameters

Model	Material	Parameter	25 °C	35 °C	45 °C
Pseudo-first order	WB-600	q_e (mg/g)	24.33	27.32	36.26
	MWB-600	K_1 (/h)	0.0227	0.0152	0.0113
		R^2	0.5960	0.6239	0.5650
		q_e (mg/g)	24.72	31.92	39.82
		K_1 (/h)	0.0253	0.0119	0.0088
		R^2	0.6149	0.5377	0.5497
Pseudo-second order	WB-600	q_e (mg/g)	67.84	69.49	70.27
	MWB-600	K_2 (g/(mg h))	0.0637	0.0818	0.0912
		R^2	0.9998	0.9999	0.9999
		q_e (mg/g)	69.44	69.88	70.37
		K_2 (g/(mg h))	0.0613	0.1084	0.1086
		R^2	0.9998	0.9999	0.9999

and the randomness of the solid–liquid interface was incremental through adsorption. These findings were consistent with previous studies [37, 38]. These obtained results showed that WB-600 and MWB-600 adsorbents could be applied to remove Cr(VI) from wastewater.

3.4 Regeneration Performance and Adsorption Cr(VI) Mechanism

To explore the regeneration property of WB-600 and MWB-600 adsorbents, the regeneration performance was investigated, and the corresponding results are presented in Fig. 6A. From Fig. 6A, after the 1st cycle to 5th cycle, the Cr(VI) removal rate was ranged from 89.42 to 81.45% for the WB-600 material, while Cr(VI) removal rate was ranged from 92.76 to 85.31% for the MWB-600 material, indicating that the WB-600 and MWB-600 adsorbents have excellent recycling ability. XRD spectra of WB-600 and MWB-600 before and after adsorption Cr(VI) are presented in Fig. 6B. After adsorption, and some new peaks emerged near 34.4° and 36.8° suggested formation of Cr_2O_3. Usually at pH 2–4, Cr(VI) can be reduced to Cr(III) by carbon material, which could act as the electron donor. Cr(III) was further coprecipitated to form Cr_2O_3 [23, 39]. The transformation processes can be expressed as following Eqs. (15), (16), (17) and (18):

$$Cr_2O_7^{2-} + 14H^+ + 6e \rightarrow 2Cr^{3+} + 7H_2O \qquad (15)$$

$$Cr_2O_7^{2-} + H_2O \rightarrow 2HCrO_4^- \qquad (16)$$

$$HCrO_4^- + 7H^+ + 3e \rightarrow Cr^{3+} + 4H_2O \qquad (17)$$

$$CrO_4^{2-} + 8H^+ + 3e \rightarrow Cr^{3+} + 4H_2O \qquad (18)$$

The adsorption Cr(VI) mechanism is presented in Fig. 6C. Firstly, the specific surface area of MWB-600 increased after being activated by KOH, and the number of active sites

Table 4 Comparison of the adsorption capacities of WB and MWB materials toward the removal of Cr(VI) with other biochar materials

| Adsorbent	pH	q_e (mg/g)	Ref
FeCl$_3$ modified biochar	2.0	47.72	[40]
ZnCl$_2$ modified hydrochar	5.0	14.0	[41]
AlCl$_3$ modified hydrochar	5.0	12.3	[41]
KOH modified biochar	2.0	29.5–34.1	[42]
KOH modified hydrochar	2.0	45.9	[43]
Biochar from Azadirachta indica leaves	2.0	58.54	[44]
Biochar from switch grass	–	49.9	[45]
WB-600	3.0	99.60	This work
MWB-600	3.0	104.17	This work

and oxygen-containing functional groups that could adsorb Cr(VI) greatly increased. Cr(VI) was adsorbed on the some protonated groups of WB-600 or MWB-600, and caused it to become positively charged by electrostatic interaction. Secondly, Cr (VI) and reduced Cr (III) can be adsorbed on the surface of WB-600 or MWB-600 materials through coprecipitation, complexation (with -OH and -COOH) or pore structure.

Table 4 lists the comparison of other previously reported adsorbents, WB and MWB materials toward the removal of Cr(VI). The prepared WB and MWB materials had bigger adsorption capacity than those other biochar materials. It is concluded that WB and MWB materials are the ideal adsorbents for removing heavy metals such as Cr(VI) from effluents.

4 Conclusion

In this work, we reported the use of biochar (WB) and modified biochar using KOH modifier (MWB) obtained

Fig. 6 Recycling performance (**A**), XRD spectra (**B**) of WB-600 (a and b) and MWB-600 (c and d) before and after Cr(VI) adsorption and Cr(VI) adsorption mechanisms (**C**) by adsorbent (Cr(VI) solution: 150 mg/L, adsorbent dosage: 2.0 g/L, *T*: 25 °C, pH: 3.0, *t*: 8 h)
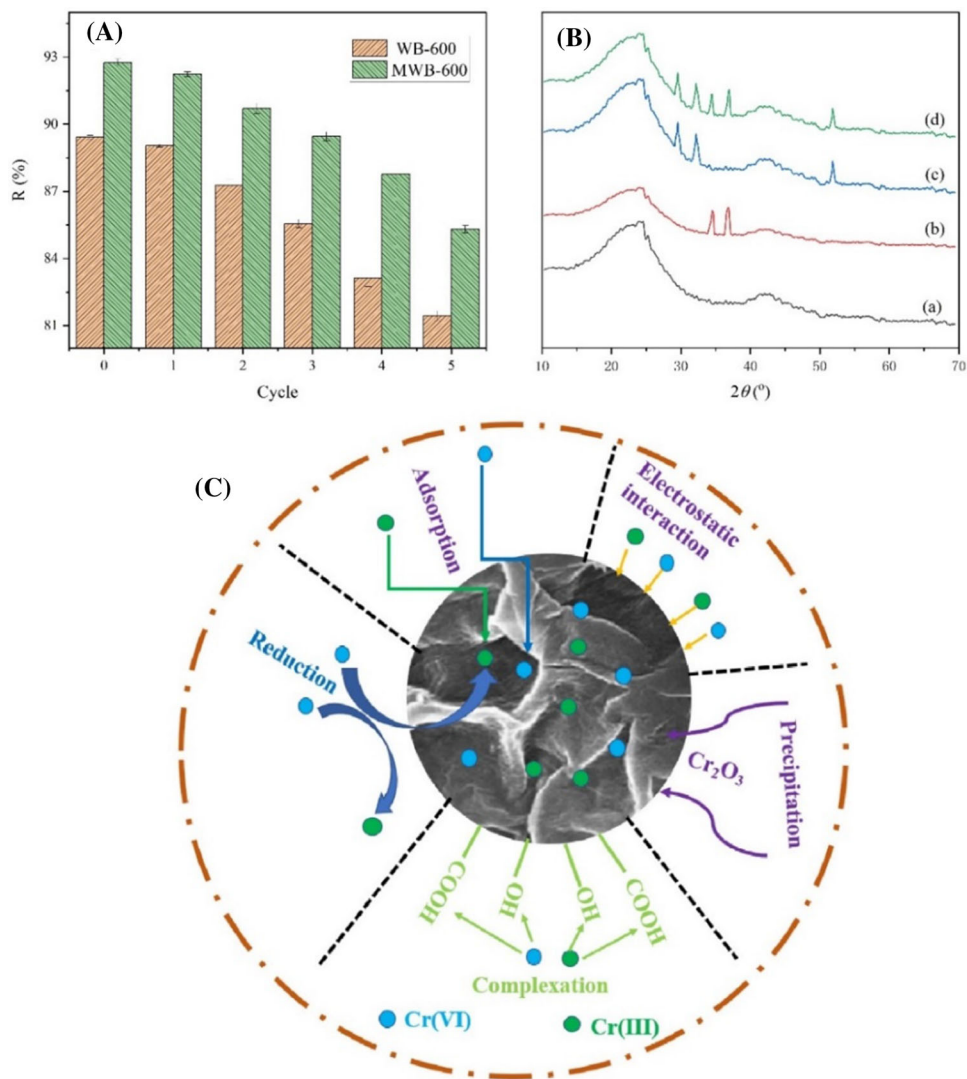
from watermelon peel as the bioresource for the removal heavy metal chromium ion from synthetic waste water. The as-prepared WB and MWB materials showed excellent adsorption capacities toward Cr(VI). At pH = 3.0, the obtained maximum adsorption capacities of WB-600 and MWB-600 were 99.60 and 104.17 mg/g, respectively. The adsorption systems were well described by pseudo-second-order model, and the adsorption process was endothermic and spontaneous. The prepared modified MWB showed excellent reusability. The obtained modified MWB materials can apply to remove heavy metal chromium ion from wastewater system.

Declarations

Conflict of interest The authors declare that they have no conflict of interest.

References

1. Hosseini, S.M.; Moradi, F.; Farahani, S.K.; Bandehali, S.; Parvizian, F.; Ebrahimi, M.; Shen, J.N.: Carbon nanofibers/chitosan nanocomposite thin film for surface modification of poly(ether sulphone) nanofiltration membrane. Mater. Chem. Phys. **269**, 124720 (2021)

2. Wang, C.; Li, X.; Wu, W.; Chen, G.; Tao, J.: Removal of cadmium in water by potassium hydroxide activated biochar produced from Enteromorpha prolifera. J. Water Process Eng. **42**, 102201 (2021)

3. Saravanan, A.; Sundararaman, T.R.; Jeevanantham, S.; Karishma, S.; Kumar, P.S.; Yaashikaa, R.: Effective adsorption of Cu(II) ions on sustainable adsorbent derived from mixed biomass (*Aspergillus campestris* and agro waste): optimization, isotherm and kinetics study. Groundw. Sustain. Dev. **11**, 100460 (2020)

4. Wu, G.; Liu, Q.; Wang, J.; Zhang, Y.; Yu, C.; Bian, H.; Hegazy, M.; Han, J.; Xing, W.: Facile fabrication of Bi$_2$WO$_6$/biochar composites with enhanced charge carrier separation for photodecomposition of dyes. Colloid Surface A **634**, 127945 (2022)

5. Long, L.; Iqbal, J.; Zhu, Y.; Zhang, P.; Chen, W.; Bhatnagar, A.; Du, Y.: Chitosan/Ag-hydroxyapatite nanocomposite beads as a potential adsorbent for the efficient removal of toxic aquatic pollutants. Int. J. Biol. Macromol. **120**, 1752–1759 (2018)

6. Dong, H.; Zhang, L.; Shao, L.; Wu, Z.; Zhan, P.; Zhou, X.; Chen, J.: Versatile strategy for the preparation of woody biochar with oxygen-rich groups and enhanced porosity for highly efficient Cr(VI) removal. ACS Omega **7**, 863–874 (2022)

7. Wu, G.; Liu, Q.; Wang, J.; Xia, S.; Huang, X.; Han, J.; Xing, W.: Construction of hierarchical Bi$_2$WO$_6$/ZnIn$_2$S$_4$ heterojunction for boosting photocatalytic performance in degradation of organic compounds and reduction of hexavalent chromium. Colloid Surface A **653**, 130048 (2022)

8. Nezamzadeh-Ejhieh, A.; Shahanshahi, M.: Modification of clinoptilolite nano-particles with hexadecylpyridynium bromide surfactant as an active component of Cr(VI) selective electrode. J. Ind. Eng. Chem. **19**, 2026–2033 (2013)

9. Kabir, M.M.; Akter, M.M.; Khandaker, S.; Gilroyed, B.H.; Didarul-Alam, Md.; Hakim, M.; Awual, Md.R.: Highly effective agrowaste based functional green adsorbents for toxic chromium (VI) ion removal from wastewater. J. Mol. Liq. **347**, 118327 (2022)

10. Rajapaksha, A.U.; Selvasembian, R.; Ashiq, A.; Gunarathne, V.; Ekanayake, A.; Perera, V.O.; Wijesekera, H.; Mia, S.; Ahmad, M.; Vithanage, M.; Ok, Y.S.: A systematic review on adsorptive removal of hexavalent chromium from aqueous solutions: Recent advances. Sci. Total Environ. **809**, 152055 (2022)

11. Yang, J.; Song, Y.; Yue, Y.; Liu, W.; Che, Q.; Chen, H.; Ma, H.: Chemically dual-modified biochar for the effective removal of Cr (VI) in solution. Polymers **14**, 39 (2022)

12. Foong, C.Y.; Zulkifli, M.F.M.; Wirzal, M.D.H.; Bustam, M.A.; Nor, L.H.M.; Saad, M.S.; Abd Halim, N.S.: COSMO-RS prediction and experimental investigation of amino acid ionic liquid-based deep eutectic solvents for copper removal. J. Mol. Liq. **333**, 115884 (2021)

13. Liu, H.; Li, P.; Zhang, T.; Zhu, Y.; Qiu, F.: Fabrication of recyclable magnetic double-base aerogel with waste bioresource bagasse as the source of fiber for the enhanced removal of chromium ions from aqueous solution. Food Bioprod. Process. **119**, 257–267 (2020)

14. Xing, W.; Liu, Q.; Wang, J.; Xia, S.; Ma, L.; Lu, R.; Zhang, Y.; Huang, Y.; Wu, G.: High selectivity and reusability of biomass-based adsorbent for chloramphenicol removal. Nanomaterials **11**, 2950 (2021)

15. Rajapaksha, A.U.; Alam, M.S.; Chen, N.; Alessi, D.S.; Igalavithana, A.D.; Tsang, D.C.W.; Ok, Y.S.: Removal of hexavalent chromium in aqueous solutions using biochar: chemical and spectroscopic investigations. Sci. Total Environ. **625**, 1567–1573 (2018)

16. Shakya, A.; Agarwal, T.: Removal of Cr(VI) from water using pineapple peel derived biochars: adsorption potential and reusability assessment. J. Mol. Liq. **293**, 111497 (2019)

17. Pap, S.; Bezanovic, V.; Radonic, J.; Babic, A.; Saric, S.; Adamovic, D.; Sekulic, M.: Synthesis of highly-efficient functionalized biochars from fruit industry waste biomass for the removal of chromium and lead. J. Mol. Liq. **268**, 315–325 (2018)

18. Guo, N.; Lv, X.; Yang, Q.; Xu, X.; Song, H.: Effective removal of hexavalent chromium from aqueous solution by ZnCl$_2$ modified biochar: effects and response sequence of the functional groups. J. Mol. Liq. **334**, 116149 (2021)

19. Peng, Z.; Zhao, H.; Lyu, H.; Wang, L.; Huang, H.; Nan, Q.; Tang, J.: UV modification of biochar for enhanced hexavalent chromium removal from aqueous solution. Environ. Sci. Pollut. Res. **25**, 10808–10819 (2018)

20. Sun, C.; Chen, T.; Huang, Q.; Zhan, M.; Li, X.; Yan, J.: Activation of persulfate by CO$_2$-activated biochar for improved phenolic pollutant degradation: performance and mechanism. Chem. Eng. J. **380**, 122519 (2020)

21. Tayibi, S.; Monlau, F.; Fayoud, N.; Oukarroum, A.; Zeroual, Y.; Hannache, H.; Barakat, A.: One-pot activation and pyrolysis of Moroccan Gelidium sesquipedale red macroalgae residue: production of an efficient adsorbent biochar. Biochar **1**, 401–412 (2020)

22. Wang, L.; Bolan, N.; Tsang, D.; Hou, D.: Green immobilization of toxic metals using alkaline enhanced rice husk biochar: effects of pyrolysis temperature and KOH concentration. Sci. Total Environ. **720**, 137584 (2020)

23. Shi, Y.; Shan, R.; Lu, L.; Yuan, H.; Jiang, H.; Zhang, Y.; Chen, Y.: High-efficiency removal of Cr(VI) by modified biochar derived from glue residue. J. Clean. Prod. **254**, 119935 (2020)

24. Wu, G.; Liu, Q.; Wang, J.; Xia, S.; Wu, H.; Zong, J.; Han, J.; Xing, W.: Facile fabrication of rape straw biomass fiber/β-CD/Fe$_3$O$_4$ as adsorbent for effective removal of ibuprofen. Ind. Crops Prod. **173**, 114150 (2021)

25. Yuan, J.; Zhu, Y.; Wang, J.; Gan, L.; He, M.; Zhang, T.; Li, P.; Qiu, F.: Preparation and application of Mg–Al compositeoxide/coconut shell carbon fiber for effective removal of phosphorus from domestic sewage. Food Bioprod. Process. **126**, 293–304 (2021)

26. Sharma, R.K.; Wooten, J.B.; Baliga, V.L.; Lin, X.; Chan, W.G.; Hajaligol, M.R.: Characterization of chars from pyrolysis of lignin. Fuel **83**, 1469–1482 (2004)

27. Schwanninger, M.; Rodrigues, J.C.; Pereira, H.; Hinterstoisser, B.: Effects of short-time vibratory ball milling on the shape of FT-IR spectra of wood and cellulose. Vib. Spectrosc. **36**, 23–40 (2004)

28. Chen, B.; Zhou, D.; Zhu, L.: Transitional adsorption and partition of nonpolar and polar aromatic contaminants by biochars of pine needles with different pyrolytic temperatures. Environ. Sci. Technol. **42**, 5137–5143 (2008)

29. Noiroj, K.; Intarapong, P.; Luengnaruemitchai, A.; Jai-In, S.: A comparative study of KOH/Al$_2$O$_3$ and KOH/NaY catalysts for biodiesel production via transesterification from palm oil. Renew. Energy **34**, 1145–1150 (2009)

30. Liu, Z.G.; Han, G.H.: Production of solid fuel biochar from waste biomass by low temperature pyrolysis. Fuel **158**, 159–165 (2015)

31. Nezamzadeh-Ejhieh, A.; Raja, G.: Modification of nanoclinoptilolite zeolite with hexadecyltrimethylammonium surfactant as an active ingredient of chromate-selective membrane electrode. J. Chem. **2013**, 1–13 (2012)

32. Liu, J.; Yang, X.; Liu, H.; Cheng, W.; Bao, Y.: NaOH activation and its adsorption mechanisms for removal of Cu(II) from aqueous solution. Colloid Surface A **601**, 124960 (2020)

33. Yuan, J.; Zhu, Y.; Wang, J.; Liu, Z.; Wu, J.; Zhang, T.; Li, P.; Qiu, F.: Agricultural bamboo leaf waste as carbon precursor for the preparation of Cu-Al/biomass fiber adsorption and its application in the removal of ammonia nitrogen pollutants from domestic wastewater. J. Wood Chem. Technol. **41**, 137–149 (2021)

34. Zhu, Y.; Rong, J.; Mao, K.; Yang, D.; Zhang, T.; Qiu, F.; Pan, J.; Pu, Z.: Boronate affinity-modified magnetic β-cyclodextrin polymer for selective separation and adsorption of shikimic acid. J. Mater. Sci. **56**, 13043–13055 (2021)

35. Yuan, J.; Zhu, Y.; Wang, J.; Liu, Z.; He, M.; Zhang, T.; Li, P.; Qiu, F.: Facile modification of biochar derived from agricultural straw waste with effective adsorption and removal of phosphorus from domestic sewage. J. Inorg. Organom. Polym. Mater. **31**, 3867–3879 (2021)

36. Zhu, Y.; Wang, K.; Lu, J.; Pan, Z.; Rong, J.; Zhang, T.; Yang, D.; Pan, J.; Qiu, F.: Teamed boronate affinity-functionalized Zn-MOF/PAN-derived molecularly imprinted hollow carbon electrospinning nanofibers for selective adsorption of shikimic acid. ACS Appl. Mater. Interface **14**, 27294–27308 (2022)

37. Liu, L.; Liu, X.; Wang, D.; Lin, H.; Huang, L.: Removal and reduction of Cr(VI) in simulated wastewater using magnetic biochar prepared by co-pyrolysis of nano-zero-valent iron and sewage sludge. J. Clean. Prod. **254**, 120562 (2020)

38. Zhang, H.; Xiao, R.; Li, R.; Ali, A.; Chen, A.; Zhang, Z.: Enhanced aqueous Cr(VI) removal using chitosan-modified magnetic biochars derived from bamboo residues. Chemosphere **261**, 127694 (2020)

39. Ding, W.; Peng, W.; Zeng, X.; Tian, X.: Effects of phosphorus concentration on Cr(VI) sorption onto phosphorus-rich sludge biochar. Front. Environ. Sci. Eng. **8**, 379–385 (2014)

40. Liang, J.; Chen, Y.; Cai, M.; Gan, M.; Zhu, J.: One-pot pyrolysis of metal-embedded biochar derived from invasive plant for efficient Cr(VI) removal. J. Environ. Chem. Eng. **9**, 105714 (2021)

41. Li, F.; Zimmerman, A.R.; Hu, X.; Gao, B.: Removal of aqueous Cr(VI) by Zn- and Al-modified hydrochar. Chemosphere **260**, 127610 (2020)

42. Khushk, S.; Zhang, L.; Pirzada, A.M.; Irfan, M.; Li, A.: Cr(VI) heavy metal adsorption from aqueous solution by KOH treated hydrochar derived from agricultural wastes. AIP Conf Proc **2119**, 020003 (2019)

43. Zhang, X.; Zhang, L.; Li, A.: Eucalyptus sawdust derived biochar generated by combining the hydrothermal carbonization and low concentration KOH modification for hexavalent chromium removal. J. Environ. Manag. **206**, 989–998 (2018)

44. Thangagiri, B.; Sakthivel, A.; Jeyasubramanian, K.; Seenivasan, S.; Raja, J.D.; Yun, K.: Removal of hexavalent chromium by biochar derived from Azadirachta indica leaves: batch and column studies. Chemosphere **286**, 131598 (2020)

45. Mishra, A.; Gupta, B.; Kumar, N.; Singh, R.; Varma, A.; Thakur, I.S.: Synthesis of calcite-based bio-composite biochar for enhanced biosorption and detoxification of chromium Cr (VI) by Zhihengliuella sp. ISTPL4. Bioresour. Technol. **307**, 123262 (2020)